DOI: 10.24996/ijs.2024.65.9.19

ISSN: 0067-2904

Construction of Multi-Channel Radio Frequency Plasma Jet System in Atmospheric Pressure and the Diagnosis of Plasma Parameters and I-V Characteristics

Waleed Ibrahim Yaseen*[1], Aseel Kamel Abd[2]
[1]*Department of Astronomy and Space College of Science University of Baghdad, Iraq, Baghdad*
[2]*Department of Physics College of Science University of Baghdad, Iraq, Baghdad*

Received: 26/11/2022 Accepted: 15/8/2023 Published: 30/9/2024

Abstract

In order to produce cold plasma at atmospheric pressure, a multi-channel RF, of (1, 2, 3, and 4 MHz) frequencies, plasma jet system is developed using argon as the working gas. This system consists of two parts, a multi-channel power supply (of a power of 100 W) and a plasma jet. A strong electric field is created that ionizes and excites argon ions. The I-V characteristics of the system and the electron temperature and density for different powers (20, 50, 70, and 80 W), gas flow rates (10, 20, 30, and 40 sccm) (standard centimeter cubic per minute) at different frequencies (1, 2, 3, and 4 MHz) are studied, using the optical emission spectroscopy method. This system can be used in medical applications and material treatment with high efficiency.

Keywords Multi-Channel Radio frequency (RF), power supply, plasma jet, Optical emission spectroscopy (OES), Argon gas (Ar).

بناء منظومة بلازما نفث متعدد القنوات للترددات الراديوية في الضغط الجوي ، وتشخيص معلمات البلازما ، وخصائص I–V

وليد ابراهيم ياسين*[1] ,اسيل كامل عبد[2]
[1]قسم الفلك والفضاء, كلية العلوم, جامعة بغداد, بغداد, العراق
[2]قسم الفيزياء, كلية العلوم, جامعة بغداد, بغداد, العراق

الخلاصه

من أجل إنتاج بلازما باردة عند الضغط الجوي ، تم تطوير نظام نفاث بلازما متعدد القنوات (1 و 2 و 3 و 4 ميجاهرتز) والغاز المستخدم هو غاز الأرجون. يتكون هذا النظام من جزأين ، مزود طاقة متعدد القنوات بقدرة 100 واط ومنظومة نفث بلازما.حيث يتم إنشاء مجال كهربائي قوي يؤين ويثير أيونات الأرجون. تم دراسة خصائص I–V للمنظومة وحساب درجة حرارة الإلكترون وكثافته لطاقات مختلفة 20 و 50 و 70 و 80 واط وبمعدلات تدفق غاز مختلفة 10 و 20 و 30 و 40 متر مكعب في المتر المربع وترددات مختلفة 1 و 2 و 3 و 4 ميجا هرتز باستخدام طريقة التحليل الطيفي للانبعاثات الضوئية. يمكن استخدام هذا النظام في تطبيقات المجال الطبي ومعالجة المواد بكفاءة عالية.

***Email:** waleedib1972cnc@gmail.com

1. Introduction

Plasma makes up more than 99% of the observable universe. Plasma can be seen in various night sky phenomena, e.g. the twinkling of stars, nebulas, auroras, and our Sun [1]. Plasma is often categorized, according to its temperature, into two categories: cold and hot [2]. Plasma sources that operate at atmospheric pressure and mild gas temperatures under non-equilibrium conditions are known as non-equilibrium plasma jet devices. They are also known as non-thermal, low-temperature, or cold plasma jets or torches [3]. As a result of extensive research efforts in recent decades, atmospheric pressure plasma jets now stand out as the most promising discharge possibilities for biological treatment operated close to room temperature and run at a moderate voltage with a modest current [4]. They are used for surface treatment of a variety of materials [5] and to cleanse mold on the surface of food [6] [7]. The atmospheric pressure plasma jet system enables the construction of tiny and affordable plasma sources since it does not need a vacuum chamber [8]. There are many different methods to generate and obtain plasma experimentally, including microwave discharge and radio frequency (RF) discharge [9], dielectric barrier discharge (DBD) [10], and direct current (DC) discharge [11] [12]. Several devices that produce a cold plasma plume in the air at atmospheric pressure have been developed in recent years. Different designs have been researched for use in medical applications and for their possibility to treat heat-sensitive surfaces [13].

A plasma jet has the shape of an uninterrupted flow when it is operating at high frequencies. The plasma jet, however, has been shown to consist of separate ionization wavefronts travelling significantly faster than the gas velocity when operating at low frequencies [14]. Many jet devices can produce plasma effluent with a length of up to tens of centimeters in the open air [15], and some can produce multiple plasma jets at once for extensive treatments [16]. Kim et al. recently created a small plasma jet whose size of 15 μm is at the level of a single cell to be used in cancer treatment [17]. Tudoran (2009) designed an RF plasma demonstration unit to generate high-frequency plasma under atmospheric pressure [18]. Surducan et al. (2011) presented a new laboratory-made plasma treatment system. The power source which generates the plasma is based on a modern half-bridge type inverter circuit working at a frequency of 4 MHz giving an output power of about 200 W [19]. Underwater corona discharge is a good, low-cost, and environmentally acceptable method for cleaning up contaminated water [20].

Knowing the plasma parameters is essential to efficiently utilize plasma in industrial, biomedical, and environmental applications. There are a few diagnostic methods for micro plasmas, and for the electron temperature measurement; in particular, a straightforward method based on optical emission which is very useful given the challenges of other existing methods using different techniques, such as the Langmuir probe [21] and Thomson scattering [22]. An atmospheric low-temperature plasma jet was studied using relative and absolute optical emission spectroscopy (OES) as a diagnostic tool for electron temperatures and electron density [23]. The electrical performance of the discharge was also studied using voltage and current probes. In this work, a multi-channel RF plasma power supply was built to operate in class A for the generation of RF plasma.

2. Multi-Channel RF Plasma Power Supply

RF power circuits that have expressly been built for the use in conventional power amplifiers to operate at several MHz are typically operated in class A or class C. to perform well at such high frequencies, these devices often employ specialized manufacturing procedures to lower the stray capacitances to accepted values. The plasma system described in this work was constructed exclusively from widely accessible general-purpose components at

low prices. Standard switch-mode power MOSFETs, however, face significant difficulties in switching effectively at 1, 2, 3, and 4 MHz because of the high capacitance of the gate. This is especially detrimental for equipment operating at high voltage and high frequency since the accumulated charge might be rather large [24]. RF power supply is composed of many parts, as shown in the block diagram of Figure 1: a multi-crystal oscillator tuned to 1, 2, 3, and 4 MHz, a high current MOSFET driver, a MOSFET power stage, and the 1, 2, 3, and 4 MHz Tesla resonator. The power supply has three outputs: 0 to +150 V for the MOSFET power stage, +5 V for the crystal oscillator, and +12 V for the driver stage. The distortion signal is eliminated at the low voltage output using the filter circuit.

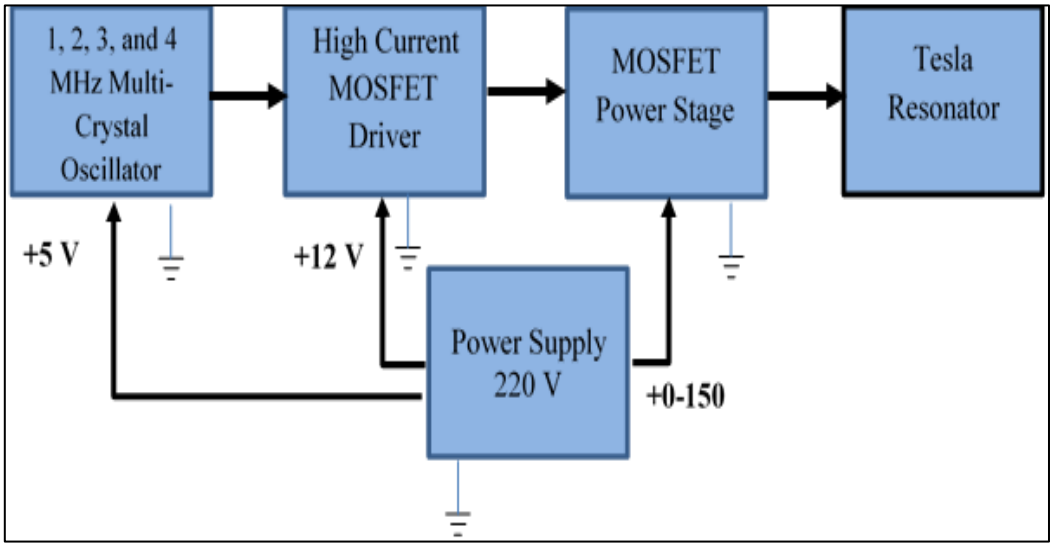

Figure 1: The multi-channel radio frequency power supply diagram.

3. Optical Emission Studies

The optical Emission Spectroscopy (OES) technique is used to determine the plasma composition and temperature of electrons (T_e). A Thorlabs optics HR-4000 spectrometer was employed to capture the emission spectrum from which the emission lines were detected between 310 and 710 nm wavelengths. An optical cable was used to feed the spectrometer's entry slit with the light from plasma spectrum, which is observed normal to the plume expansion. Utilizing the spectrometer's measurements of atomic emission, line intensity T_e and reactive species were measured. The Boltzmann plot approach was used to extract T_e from the spectral data. [25].

$$\ln\left(\frac{I_n\lambda_n}{g_nA_n}\right) = -\frac{E_n}{T_e} + C \qquad (1)$$

Where: T_e is the excited electron temperature, A_n is the transition probability, I_n is the intensity of the spectral line of wavelength λ_n, g_n is the statistical weight factor, E_n is the energy of the excited states of the spectral line, and C is a constant, which was neglected in the current study. The spectral lines' intensity was determined from the observed spectra. The NIST atomic spectra database was used to determine the values of E_n, g_n, and A_n for the chosen lines [26].

The electron density may be determined using the Stark-broadening of spectral lines, which, in our case, predominates over the spectral line width of Doppler, collisional, or instrumental broadening. The full-width at half maximum (FWHM) (denoted as $\Delta\lambda_{\frac{1}{2}}$)of the Stark-broadened line determined by Equation 2, and is proportional to the electron density [27]:

$$\Delta\lambda_{\frac{1}{2}} = 2\omega\left(\frac{n_e}{10^{16}}\right) \qquad (2)$$

Where|; ω is the impact broadening factor and n_e is the electron density (cm^{-3}). The impact factor was obtained from the study of Konjevic et al. [28].

4. Experimental Setup

Two electrodes make up the plasma jet. The first electrode is a hollow stainless steel wire 90 mm long and 1 mm diameter connected to the high voltage RF 2 MHz power source. The second electrode is placed around the end of a glass pipe, as illustrated in Figure 2, and it is connected to ground.

Four major components make up the plasma system:

1. RF high voltages power supply at 1, 2, 3, and 4 MHz frequencies 2. Plasma jet 3. Argon gas. 4. A flow meter. The plasma jet system's schematic design and photographic pictures for the RF plasma jet at various RF powers (20, 50, 70, and 80 W) are shown in Figure 2.

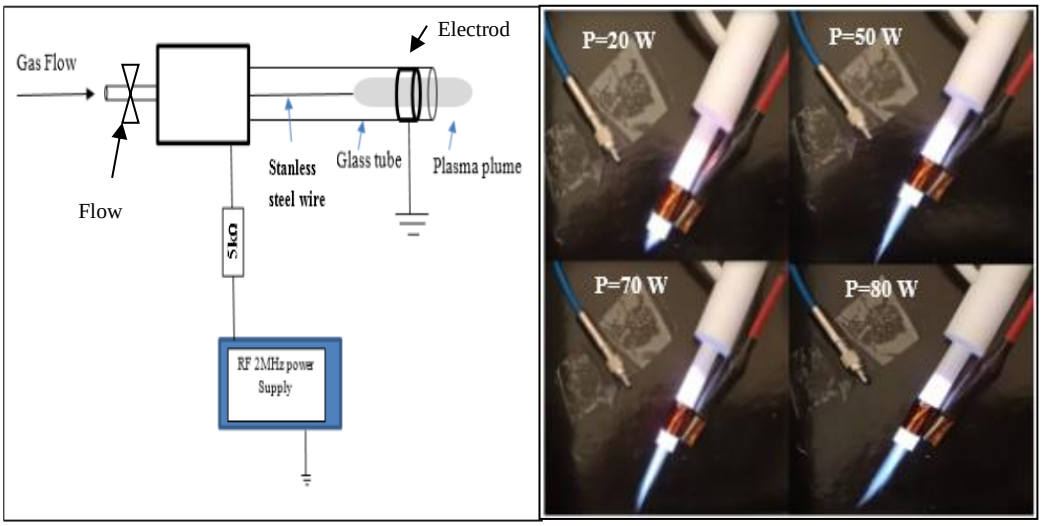

Figure 2: (a) Schematic diagram of the plasma jet system; (b) Photographic images of the RF plasma jet at various RF power levels (20, 50, 70, and 80 W).

5. Results and Discussion

5.1. Plasma Diagnosis

Figure 3 displays the plasma emission spectra at 20, 50, 70, and 80 W RF power, showing the detected significant lines at 696.5431, 706.7218, 727.2936, and 738.398 nm.

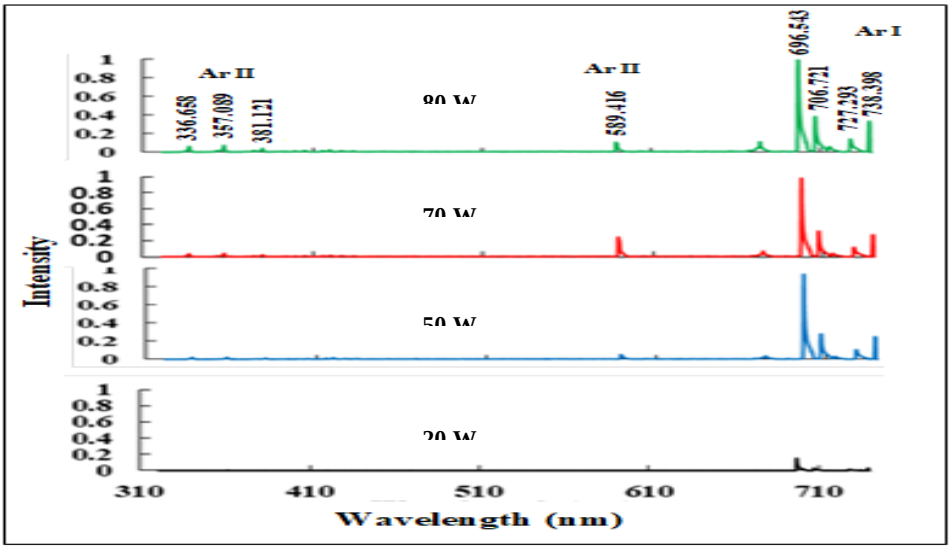

Figure 3: Plasma emission spectra at different RF powers.

The intensity change of these spectral lines was studied against the RF power values and the Ar gas flow rate. The NIST database was utilized to determine the ArI parameters. The Boltzmann plot method was employed to determine the electron temperature (Te) from these observed ArI lines.

The electron temperature (Te) and electron density (n_e)can be calculated from the spectral lines at each RF power value using Eq. (1) and (2).
Figures 4 and 5 is show the intensity change of the ArI spectral lines of the plasma emission spectra with the RF power and the Ar gas flow rate, respectively. With the flow rate remaining constant at 30 sccm it can be noted that as the power of the source increases, the ArI intensity lines grow, as a result of the rise of the ionization level and electron energy, increasing the rate of electron-neutral impact excitation. When electrons collide with other particles, they transfer their energy and so excite the particles. The ArI lines exist in the area of short wavelengths.

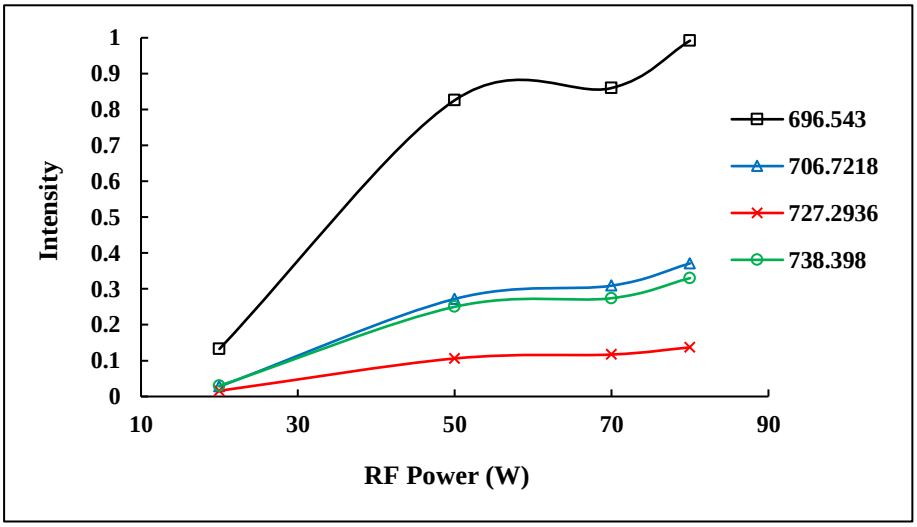

Figure 4: The ArI lines intensity vs. RF power values.

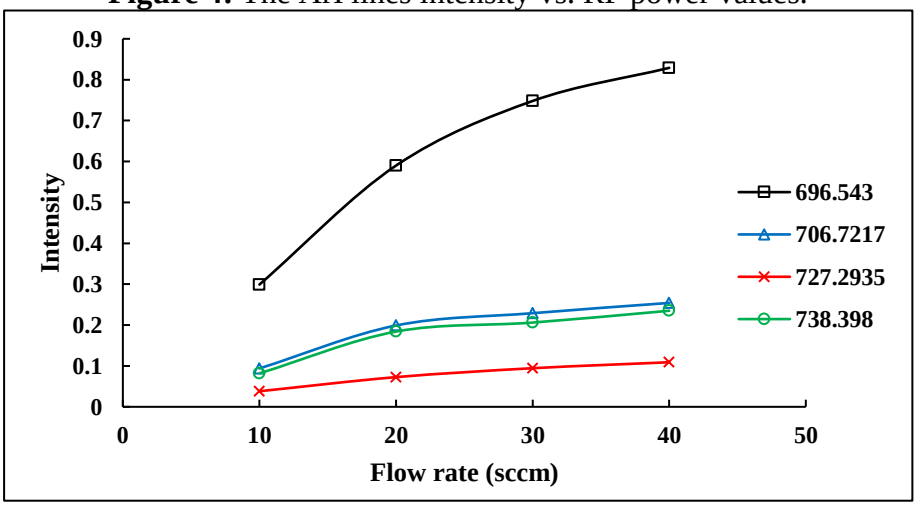

Figure 5 : The ArI lines intensity vs. argon gas flow rate (sccm).

Electron temperature and density were measured using the four ArI lines of (696.5431, 706.7218, 727.2936, and 738.398) nm wavelengths as a function of RF power, gas flow rate for different RF voltage frequencies (1, 2, 3, and 4 MHz).

Figure 6 illustrates the Boltzmann plots to determine electron temperature using the slope of the straight lines. Using Eq. (1), the electron temperature (Te) was plotted at frequency values of (1, 2, 3, and 4 MHz) as a function of RF power (20, 50, 70, and 80) W and gas flow rate (10, 20, 30, and 40), as shown in Figure7 and 8. The temperature rises with the increase of power at different frequencies, as seen in Figure 7. Increasing the feeding power, more energy is transferred to the plasma electrons; therefore, electron temperature increases and ionization rises. This is due to the fact that the increase in the electric field provides additional energy to the electrons, thus increasing their temperature. This result agrees with that of Naveed et al. [29].

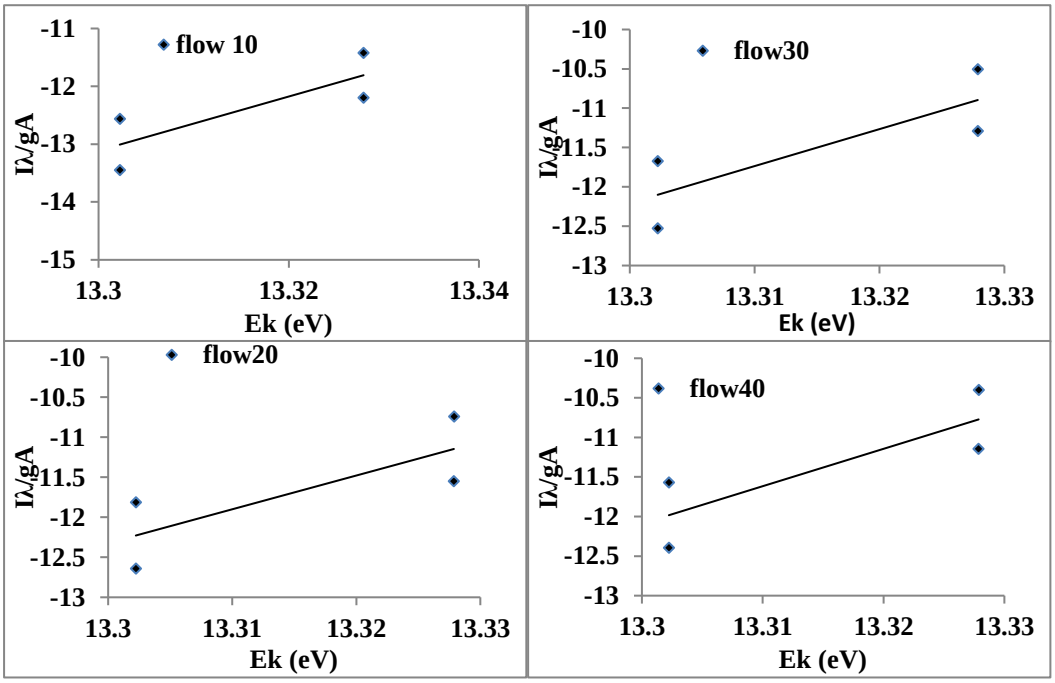

Figure 6: The Boltzmann plot utilizing the AlII ionic lines at different flow rates (10, 20, 30, and 40).

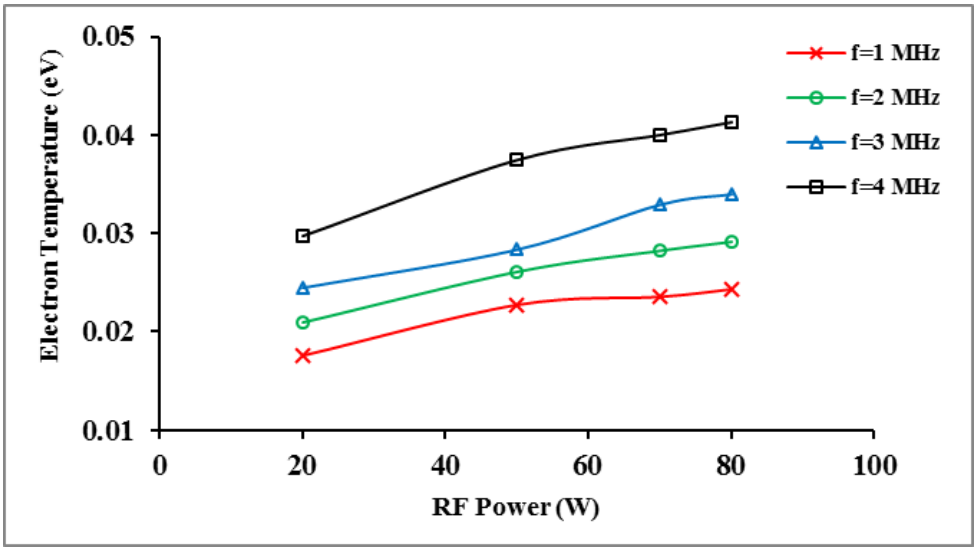

Figure 7: Variation of electron temperature with RF power at different frequency values.

Figure 8 demonstrates how the electron temperature changes with the gas flow rate at different frequencies. The temperature of the electron decreases as the flow rate rises because more argon atoms are present, and therefore the electron undergoes more collisions and thus loses more energy. The temperature at a fixed flow rate rises with increasing the frequency due to increased electron energy [30].

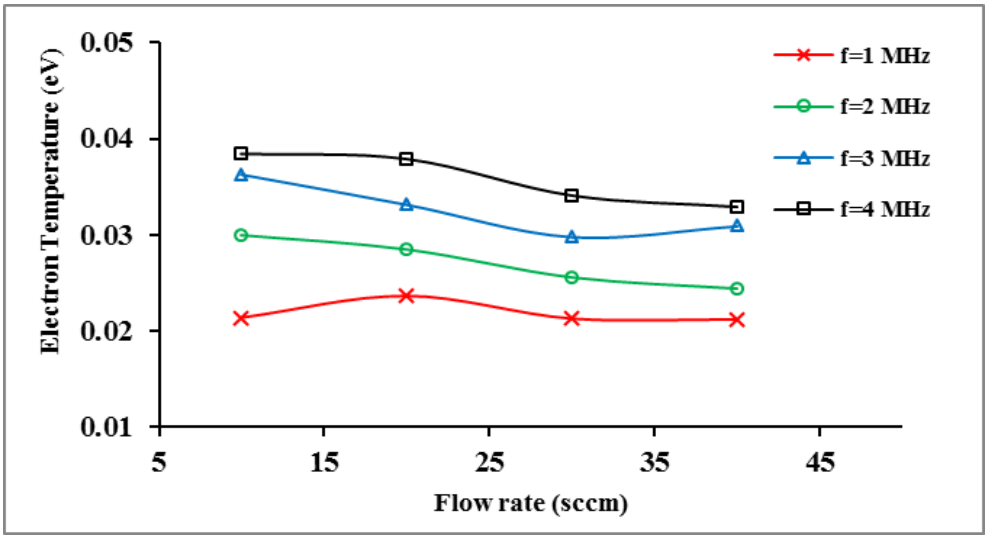

Figure 8: Variation of electron temperature with gas flow rate at different frequency values.

The electron density at the ArI 696.5 nm spectral line was calculated using Eq. (2). Figure 9 shows the change in electron density as a function of RF power at different frequencies. When the power is increased, both the electron energy and ionization level rise. As a result, the electron density grows. The increase in the frequency leads to an increase in the potential difference between the two electrodes, which leads to an increase in the electron energy and ionization; thus the electron density increase. This result agrees with that of Zheng et al. [31] .

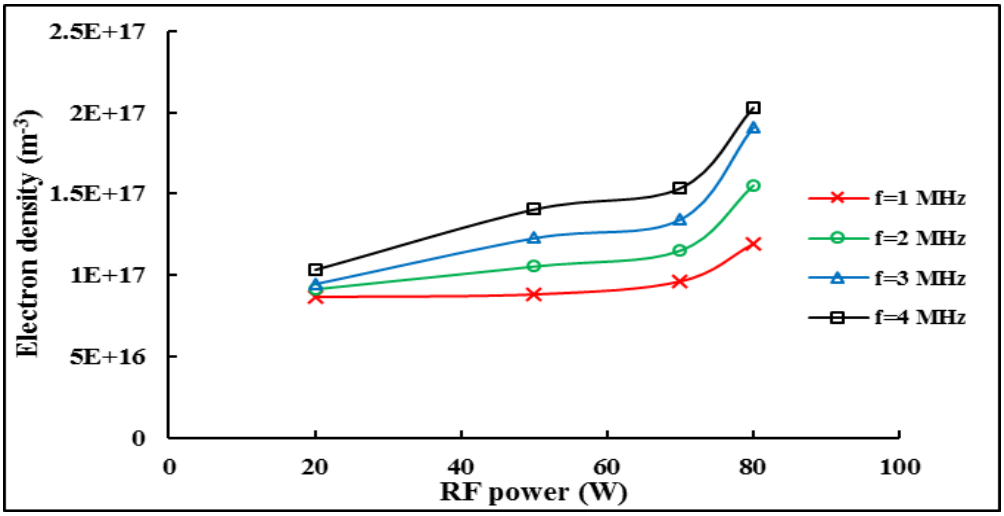

Figure 9 : The electron density variation with RF power at different values of frequency.

Figure 10 depicts the variation of electron density with gas flow rate at different frequencies. Electron density gradually increases with increasing the gas flow rate due to an increase in the number of ionized argon atoms leading to an increase in the number of electrons. These results agree with those of Hashim et al. [32] and Aadim et al. [33].

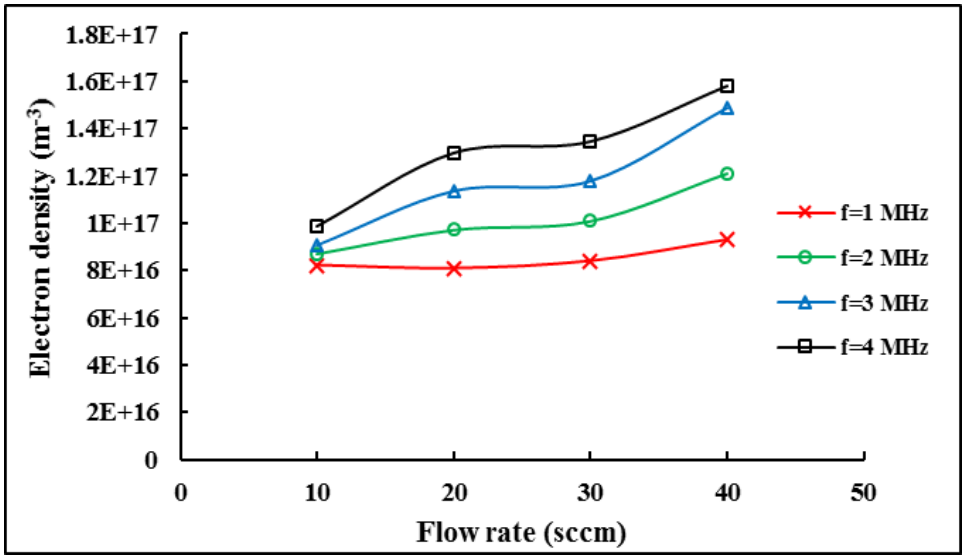

Figure 10 : Variation of electron density with flow rate at different frequency values

5.2. Determination of Output Parameters for RF Power Supply

The electronic circuit for the RF power supply operates at different voltages and is equipped with a DC power supply. This electronic circuit is divided into several stages. The first stage is a multicrystal oscillator consisting of four crystals supplying frequencies of 1, 2, 3, and 4 MHz and an oscillation circuit supplied with 5 V. In this stage, sine wave signals are obtained for all frequencies, with peak-to-peak voltages of 2.34, 1.45, 1.05 V, and 930.6 mV, respectively, as shown in Figure 11.

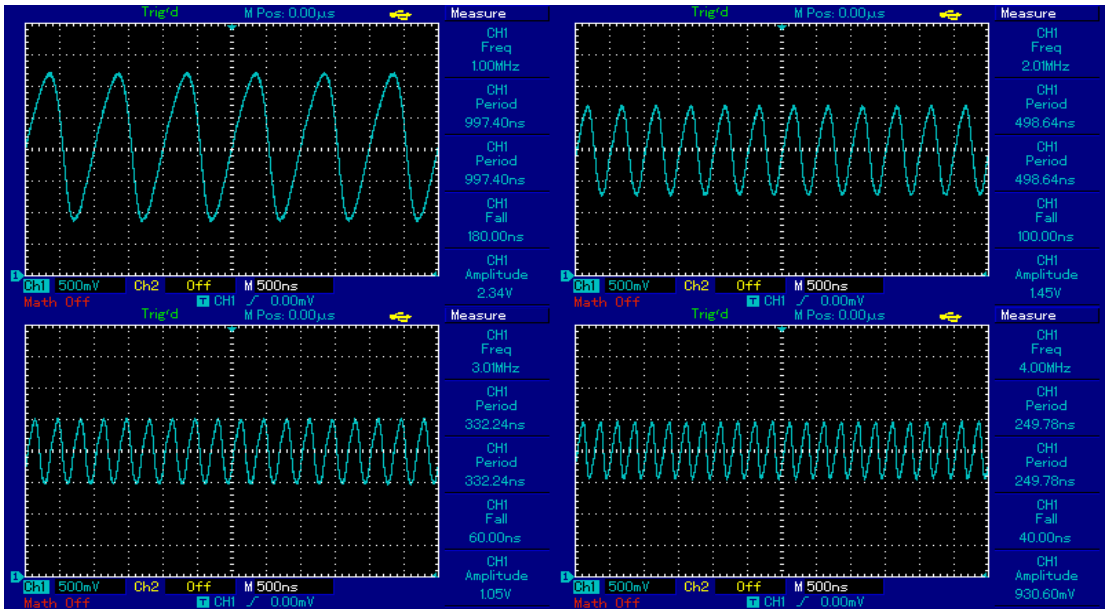

Figure 11: Sine wave signals of 1, 2, 3, and 4 MHz frequencies at the output of the first stage (oscillation stage).

The effect of frequency on the discharge parameters is also studied and detailed in Figure 12. The Positive effects of the frequency on the system's discharge current can be noted when the frequency is increased. As the frequency is increased, it was found that the discharge breakdown voltage is increased where at frequency 1 MHz the discharge voltage is 10 to 450V and discharge current 45 mA, at 2 MHz discharge voltage is 10 to 760 V, and the

discharge current is 69.3 mA, at 3 MHz discharge voltage is 10 to 860 and discharge current 78.7 mA, at 4 MHz discharge voltage 10 to 946 V and discharge current 81.6 Ma. This result agrees with that of Abd and Abbas [34].

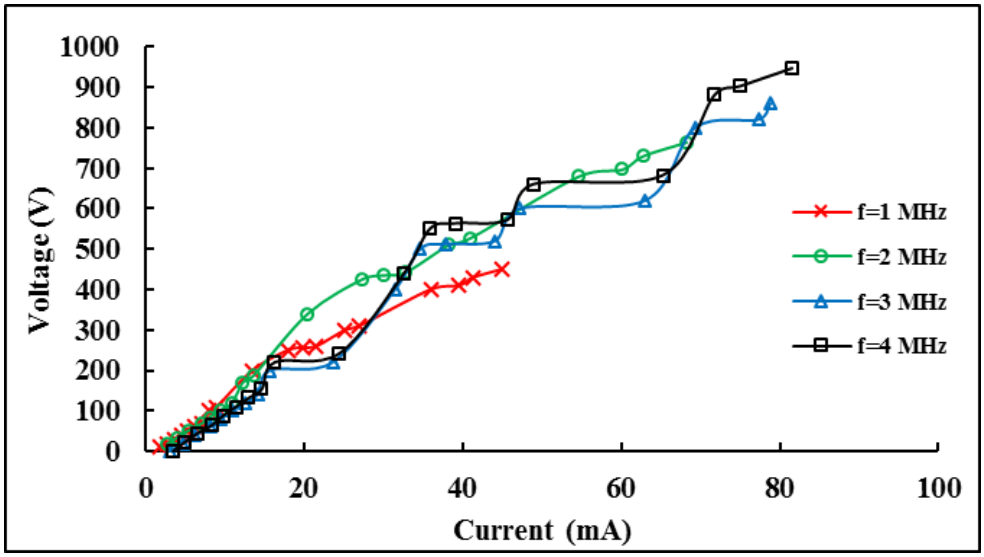

Figure 12: The I–V characteristics curves for different frequency 1, 2, 3, and 4 MHz

6. Conclusions

An RF plasma jet system operating in a frequency range of (1-4) MHz was built and tested successfully. This paper shows the effects of the power system, gas flow rate, and frequency on the plasma parameters and I-V characteristics. A positive impact on electron temperature and density at high power and frequency was noted. Through these results, this RF power supply can be used in many applications, such as generating DBD plasma and sputtering plasma. By changing the power supply frequency, insulators and semiconductors can be studied and deposited for the manufacture of electronic parts.

References

[1] R. R. Khanikar and a. H. Bailung, "Cold Atmospheric Pressure Plasma Technology for Biomedical Application," in *Plasma Science and Technology*, A. Shahzad,Ed., IntechOpen, pp. 1-21, 2022.

[2] W. I. Yaseen, A. F. Ahmed, D. A. Al-Shakarchi and A. Mutlak, "Development of a high-power LC circuit for generating arc plasma and diagnostic via optical emission spectroscopy," *Applied Physics A*, vol. 128, no. 148, pp. 1-9, 2022.

[3] F. Fanellia and F. Fracassi, "Atmospheric pressure non-equilibrium plasma jet technology: generalfeatures, specificities and applications in surface processing of materials," *Institute of Nanotechnology (NANOTEC)*, pp. 1-106, 2017.

[4] H. M. Joh, S. J. Kim, T. H. Chung and a. S. H. Leem, "Comparison of the characteristics of atmospheric pressure plasma jets using different working gases and applications to plasma-cancer cell interactions," *AIP Advances*, vol. 3, no. 9, id.092128, 2013.

[5] E. Stoffels, A. J. Flikweert, W. W. Stoffels and a. G. M. W. Kroesen, "Plasma needle: a non-destructive atmospheric plasma source for fine surface treatment of (bio)materials," *Plasma Sources Sci. Technol*, vol. 11, p. 383–388, 2002.

[6] P. Thonglor and a. P. Amnuaycheewa, "Application of atmospheric-pressure argon plasma jet for bread mold decontamination," *IOP Conf. Series: Journal of Physics: Conf. Series* , vol. 901, no. 012140, pp. 1-4, 2017.

[7] S. Bekeschus, K. Masur, J. Kolata, K. Wende, A. Schmidt, L. Bundscherer, A. Barton, A. Kramer, B. Bro¨ker and a. K.-D. Weltmann, "Human Mononuclear Cell Survival and

Proliferation is Modulated by Cold Atmospheric Plasma Jet," *Plasma Process and Polymers,* vol. 10, no. 8, pp. 706-713, 2013.

[8] O. V. Penkov, M. Khadem, W.-S. Lim and D.-E. Kim, "A review of recent applications of atmospheric pressure plasma jets for materials processing," *Journal of Coatings Technology and Research,* vol. 12, no. 2, p. 225–235, 2015.

[9] J. Tous, M. Sicha, Z. Hubicka, L. Soukup, L. Jas-trabik, M. Cada and M. Tichy, "The Radio Frequency Hollow Cathode Discharge Induced by the RF Discharge in the Plasma-Jet Chemical Reactor," *Contrib. Plasma Phys,* vol. 42, no. 1, p. 119−131, 2002.

[10] R. Brandenburg, "Corrigendum: Dielectric barrier discharges: progress on plasma sources and on the understanding of regimes and single filaments (2017 Plasma Sources," *Plasma Sources Sci. Technol.*, vol. 27, no. 7, p. 079501, 2018.

[11] X. L. Deng, A. Y. Nikiforov, P. Vanraes and a. C. Leys, "Direct current plasma jet at atmospheric pressure operating in nitrogen and air," *Journal of Applied Physics,* vol. 113, no. 023305, pp. 1-9, 2013.

[12] H. A. Sadeq and a. W. I. Yaseen, "Optical Properties of Manufactured Mirrors Using DC Plasma Magnetron Sputtering Technique," *Iraqi Journal of Science* , vol. 63, no. 5, pp. 2297-2306 , 2022.

[13] A.-A. H. Mohamed, R. O. Price, R. J. Swanson and a. A. Bowman, "Cold Atmospheric Pressure Air Plasma Jet for Medical Applications," *Applied Physics Letters* , vol. 92, no. 241501, pp. 1-4, 2008.

[14] N. Jiang and Caoa, "Atmospheric pressure plasma jet: Effect of electrode configuration, discharge behavior, and its formation mechanism," *Journal of Applied Physics,* vol. 106, no. 013308, pp. 1-7, 2009.

[15] L. XinPei, . J. ZhongHe, X. Qing and . T. ZhiYuan, "An 11cm long atmospheric pressure cold plasma plume for applications of plasma medicine," *APPLIED PHYSICS,* vol. 92, no. 081502, pp. 1-2, 2008.

[16] Q. Nie, Z. Cao, C. S. Ren, D. Z. Wang and a. M. G. Kong, "A two-dimensional cold atmospheric plasma jet array for uniform treatment of large-area surfaces for plasma medicine," *New Journal of Physics* , vol. 11, no. 115015, pp. 1-14, 2009.

[17] J. Y. Kima, Y. W. b, J. L. b and S.-O. Kim, "15-m-sized single-cellular-level and cell-manipulatable microplasma jet in cancer therapies," */ Biosensors and Bioelectronics,* vol. 2, p. 555–559, 2010.

[18] C. D. Tudoran, "Simplified portable 4 MHz RF plasma demonstration unit," in *Journal of Physics: Conference Series 182, 012034* , 2009.

[19] C. D. Tudoran, V. Surducan and a. S. D. Anghel, "High Frequency Atmospheric Cold Plasma Treatment System For Materials Surface Processing," in *AIP Conf. Proc. 1425, 106-109 (2012),* 2011.

[20] E. Stoffels, A. J. Flikweert, W. W. Stoffels and a. G. M. W. Kroesen, "Plasma needle: a non-destructive atmospheric plasma source for fine surface treatment of (bio)materials," *Plasma Sources Sci. Technol,* vol. 11, p. 383–388, 2002.

[21] A. A.-K. Hussain, K. A. Aadim and W. I. Yaseen, "Diagnostics of low-pressure capacitively coupled RF discharge argon," *Iraqi Journal of Physics* , vol. 13, no. 27, pp. 76-82, 2015.

[22] D. Mariotti, Y. Shimizu, T. Sasaki and a. N. Koshizaki, "Gas temperature and electron temperature measurements by emission spectroscopy for an atmospheric microplasma," *JOURNAL OF APPLIED PHYSICS* , vol. 101, no. 013307 , pp. 1-8, 2007.

[23] Q. Xiong, A. Y. Nikiforov, M. A. G. alez, C. Leys and a. X. P. Lu, "Characterization of an atmospheric helium plasma jet by relative and absolute optical emission spectroscopy," *Plasma Sources Sci. Technol,* vol. 22, no. 015011, pp. 1-13, 2013.

[24] Richies, "Tesla Coil Mailing List," *https://www.richieburnett.co.uk/tesla.shtml.*

[25] G. Prakash, N. Behera, K. Patel and a. A. Kumar, "Characterization of atmospheric pressure plasma plume," *arXiv preprint arXiv,* vol. 1912, no. 03691, pp. 1-11, 2019.

[26] "https://physics.nist.gov/PhysRefData/ASD/lines_form.html".

[27] H. H. Ley, A. Yahaya and a. R. K. R. Ibrahim, "Analytical Methods in Plasma Diagnostic by Optical Emission Spectroscopy: A Tutorial Review," *Journal of Science and Technology* , vol. 6, no. 1, pp. 49-66, 2014.

[28] N. Konjevic, A. Lesage, J. R. Fuhra and a. W. L. Wiese, "Experimental Stark Widths and Shifts for Spectral Lines of Neutral and Ionized Atoms," *Journal of Physical and Chemical Reference Data* , vol. 31, no. 3, pp. 819-927, 2002.

[29] M. Naveed, N. Rehman, S. H. S. Zeb and a. M. Zakaullaha, "Langmuir probe and spectroscopic studies of RF generated helium-nitrogen mixture plasma," *The European Physical Journal D,* vol. 47, p. 395–402, 2008.

[30] N. Hendawy, H. McQuaid, D. Mariotti and P. Maguire, "Continuous gas temperature measurement of cold plasma jets containing microdroplets, using a focussed spot IR sensor," *Plasma Sources Science and Technology,* vol. 29, no. 8, p. 085010, 2020.

[31] H. Zheng, J. W. J. Z. and a. X. Huang, "Diagnosis of electron density andtemperaturebyusing collisional radiative model incapacitively coupled Ar plasmas I : triple-frequency discharges," *arXiv preprint* , vol. 2010, p. 10714, 2020.

[32] I. H. Hashim, K. A. Aadim and M. R. Ali, "Effect of gas flow rate on plasma temperature and electron density of atmospheric argon plasma jet," *Iraqi Journal of Physics,* vol. 15, no. 35, pp. 117-124, 2017.

[33] K. A. Aadim, A. A.-K. Hussain, N. Kh.Abdalameer, H. A. Tawfeeq and H. H. Murbat, "Electron Temperature and Density Measurement of Plasma Jet in Atmospheric Pressure," *International Journal of Novel Research in Physics Chemistry & Mathematics,* vol. 2, no. 2, pp. 28-32, 2015.

[34] A. K. Abd and a. Q. A. Abbas, "Spectral Analysis of the Effects of Variation in Electrodes' Area for Dielectric Barrier Discharge Actuator," *Iraqi Journal of Science,* vol. 64, no. 4, pp. 1691-1703, 2023.